LOW-CHARGE TO HIGH-CHARGE BEIDELLITE CONVERSION IN A VERTISOL FROM SOUTH ITALY

Dominique Righi,[1] Fabio Terribile,[2] and Sabine Petit[1]

[1] Laboratoires de Pédologie et de Pétrologie de la surface, UA 721 CNRS
Faculté des Sciences, 86022 Poitiers, France

[2] CNR-ISPAIM, P.O. Box 101, 80040 S. Sebastiano al Vesuvio, Napoli, Italy

Abstract—The fine silt (2–5 μm) coarse clay (0.1–2 μm) and fine clay (<0.1 μm) fractions of a Vertisol from South Italy were studied with X-ray diffraction. The most reactive fine clay (<0.1 μm) fraction was investigated in detail using a curve decomposition method analysis of X-ray diffraction diagrams, FTIR spectroscopy and chemical analysis. In the soil parent material, the fine clay fraction was dominated by low-charge smectites (beidellite and montmorillonite) whereas, high-charge beidellite was the dominant clay mineral in the fine clay from the upper soil horizons. This suggested that high-charge beidellite was produced through alteration of the preexisting low-charge smectites and was the stable clay phase in this soil environment, characterized by high pH (>8.0). After K-saturation and 25 wetting and drying cycles, the high-charge beidellite from the soil horizons lost expandability far more than the original low-charge smectites.

Key Words—Beidellite, Smectites, Vertisol.

INTRODUCTION

High-charge beidellite has been reported as the dominant clay mineral in many Vertisols (Badraoui *et al* 1987, Badraoui and Bloom 1990, Wilson 1987, Kounetsron *et al* 1977, Rossignol 1983). The high tetrahedral charge in soil beidellite is generally thought to be inherited from a preexisting mica structure. During weathering soil mica would be transformed to beidellite, preserving the tetrahedral character of the charge. In base-saturated horizons with low organic matter content and high pH's (>6.7), as is the case in some Vertisols, only montmorillonite would form from dissolution and recrystallization processes (Borchart 1989). However, the development of a tetrahedral charge was observed in hydrothermally altered montmorillonite (150–250°C) (Howard and Roy 1985). Similar results were obtained by Eberl *et al* (1993) at 25 and 60°C and, in alkaline medium.

The purpose of this study was to characterize the smectite in a Vertisol developed from a highly smectitic parent-material and to relate the properties of this smectite to its genesis and stability. Soil smectites with high tetrahedral charge are believed to fix K and NH_4 more strongly than montmorillonite (Bradaoui and Bloom 1990). In relation with soil fertility and K availability for plants it is of importance to better understand the mineralogical evolution in smectite-rich soils like Vertisols.

SOIL MATERIAL

The Vertisol profile (Udic Haploxerert, Soil Survey Staff 1992) was located near the village of S. Bartolomeo in Galdo in the Campania region (Naples, Italy). In this area Vertisols have developed on remnants of high plain surfaces. The studied soil was at an elevation of 440 m and located on a gentle slightly concave slope. The parent-material, a pelitic sediment ("argille varicolori"), is rich in clays, having more than 65% clay (<2 μm). The soil profile was sampled according to five major horizons, including Ap, Bwss1, Bwss2, Bwss/Ck and Ck. A short description of the soil profile is given below, together with some important analytical data (Table 1). Colors are for the moist sample.

0–40 cm: Ap, very dark grey (10YR 3/1) clay, friable, moderate fine granular and coarse subangular blocky structure, slight HCl effervescence, smooth boundary.

40–80 cm: Bwss1, black (10YR 2/1) clay, firm, strong coarse subangular and angular blocky structure with wedge-shaped peds, slight HCl effervescence, smooth gradual boundary.

80–160 cm: Bwss2, black (10YR 2/1) clay, hard, coarse angular blocky structure with wedge shape, larger peds have distinct slickenslides, moderate HCl effervescence, irregular gradual boundary.

160–200 cm: Bwss/Ck, dark gray (10YR 4/1) clay, very firm, very coarse angular blocky and massive structure, few and very large slickensides, strong HCl effervescence, smooth diffuse boundary.

>200 cm: Ck, olive (5Y 5/3) clay, very firm, massive structure, slight HCl effervescence.

METHODS

The bulk soil samples were analyzed according to SISS (Società Italiana Scienza del Suelo 1985) methods: particle size analysis was carried out by the pipette method, cation exchange capacity (CEC) and exchangeable bases were determined by $BaCl_2$ and atomic adsorption spectrometry (AAS) respectively. Bulk chem-

Table 1. Characteristics of the soil horizons. Clays ($<2~\mu m$), $CaCO_3$, organic matter (org. matter): percent 105°C dry soil. CEC: $cmol_c~kg^{-1}$; Na^+, K^+, Ca^{2+}, Mg^{2+}: exchangeable cations.

	Depth (cm)	Clay ($<2\mu m$)	$CaCO_3$ %	Org. matter	pH (H_2O)	CEC	Na^+ %CEC	K^+ %CEC	Ca^{2+} %CEC	Mg^{2+} %CEC
Ap	0–40	66.0	0.5	2.6	8.0	40.0	0.8	3.0	85.0	11.2
Bwss1	40–80	67.6	1.0	2.4	8.1	39.8	2.1	3.1	81.2	13.6
Bwss2	80–160	67.1	9.3	1.8	8.6	40.6	6.5	2.4	71.6	19.5
Bwss/Ck	160–200	66.1	17.0	1.8	8.6	33.5	6.2	1.6	63.1	29.1
Ck	>200	66.1	1.2	0.3	8.9	53.3	15.4	1.1	53.3	30.2

ical analyses were performed according to the procedure described by Jeanroy (1972). Si, Al, Fe, Ti, Mg, Ca, Na, and K were analyzed by AAS.

The silt and clay fractions were obtained from the samples by sedimentation after destruction of organic matter with dilute, Na-acetate buffered H_2O_2 and dispersion at pH = 9 (NaOH). Decarbonatation treatment was not used to avoid possible alteration of clay minerals, induced by acidification of the medium. The clay fractions ($<2~\mu m$) were divided into fine ($<0.1~\mu m$) and coarse clay ($0.1–2~\mu m$) subfractions using a Beckman J2-21 centrifuge equiped with the JCF-Z continous flow rotor. X-ray diffraction (XRD) diagrams were obtained from parallel-oriented specimens using a Philips diffractometer with Fe-filtered $CoK\alpha$ radiation. Pretreatment of the specimens included Ca saturation and solvation with ethylene glycol, and K saturation followed by heating to 200°C. High-charge and low-charge smectite layers were identified on the basis of re-expansion with ethylene glycol after K-saturation and heating to 200°C. The Greene-Kelly (1953) test (Li saturation) was used to distinguish montmorillonite and beidellite. Randomly oriented powders were used to obtained the 060 bands and the three-dimensional reflections needed to compute the turbostratic index as proposed by Reynolds (1992). The diffractograms were recorded numerically by a DACO-MP recorder associated with a microcomputer using the Diffrac AT software (SOCABIM, France). The XRD patterns were then decomposed into their elementary component

curves using a X-ray decomposition program (DE-COMPXR, Lanson 1993). Such a decomposition allowed an improved measure of the position and relative intensity of the diffraction peaks.

FTIR spectroscopy was performed on KBr disks prepared by mixing 1 mg sample with 300 mg KBr and pressing at 13 kg/cm^2. FTIR spectra were recorded using a Nicolet 5DX spectrometer.

On the $<0.1~\mu m$ fine clay subfractions, CEC was obtained by saturation with Mg^{2+}, the excess of Mg salt ($MgCl_2$) being carefully washed out with ethanol. Mg^{2+} was then exchanged by NH_4^+ and analyzed by AAS in the exchange solution.

Wetting and drying cycles in the presence of K ions were conducted by mixing 100 ml of 1M KCl solution with 2 g of coarse clay ($0.1–2~\mu m$) in glass beakers, and then by drying them at 60°C. After drying, fresh distilled water was added, and the drying cycle repeated. Twenty-five cycles were performed. After reaction, samples were washed several times with distilled water, then saturated with Ca^{2+} in 1M $CaCl_2$ solution, and then thoroughly washed until chloride-free.

RESULTS

Soil analysis

The cumulative grain size distribution curves computed for the 20–2000 μm portion of the five horizons were quite identical (Figure 1). All the samples were heavy clays with more than 65% of the particles in the $<2~\mu m$ fraction (Table 1). Even in the parent material sample (Ck), the coarse silt and sand fractions were minor fractions, less than 15% of the whole samples. Calcium carbonate was present in increasing amounts from the Ap horizon (0.5%) to the Bwss2 horizon (17%). Sample pHs in H_2O were about 8.0 in the two upper horizons (Ap, Bwss1) and higher in the deeper horizons (8.6 to 8.9). CECs of the soil samples were comprised between 30 and more than 50 $cmol_c~kg^{-1}$. Exchangeable cations clearly indicated the increase with depth of the proportion of Mg^{2+} while K^+ and Ca^{2+} were decreased. The chemical composition of the bulk soil sample was near constant (Table 2).

X-ray diffraction

All the XRD diagrams exhibited the typical diffraction bands of smectite minerals: intense peak at about
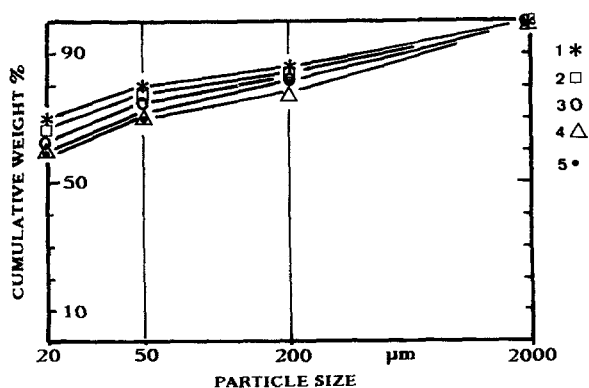

Figure 1. Cumulative grain size distribution curves. 1: Ck; 2: Bwss/Ck; 3: Bwss2; 4: Bwss1; 5: Ap.

Table 2.   Total analyses of the bulk soil samples. percent 105° dry sample; LOI: loss on ignition. (CaO percentages were corrected with reference to calcium carbonate content).

	SiO_2	Al_2O_3	Fe_2O_3	MnO	MgO	CaO	Na_2O	K_2O	TiO_2	LOI
Ap	56.88	15.44	5.98	0.19	1.74	2.31	1.38	2.34	0.91	13.67
Bwss1	55.74	15.56	5.98	0.19	1.76	2.11	1.35	2.25	0.89	13.88
Bwss2	55.18	15.67	6.01	0.21	1.79	2.75	1.44	2.23	0.88	14.22
Bwss/Ck	53.74	16.21	6.21	0.14	2.58	2.24	1.37	2.28	0.87	14.37
Ck	53.95	17.40	6.09	0.08	2.27	1.31	1.38	2.02	0.72	14.85

1.52 nm (air dry) or 1.71 nm (ethylene glycol) with higher orders at 0.876, 0.556 and 0.335 nm (ethylene glycol) (Figure 2). In the fine clay subfractions (<0.1 μm) minor proportions of illite (peak at 1.001 nm) and kaolinite (peaks at 0.720 and 0.358 nm) were associated with the smectite clays. In the coarse clay (0.1–2 μm) (not shown) and fine silt (2–5 μm) fractions (Figure 2), mica (sharp peaks at 1.004 and 0.499 nm), quartz (0.424 and 0.334 nm) and feldspars (0.325 and 0.318 nm) were also present. In the fine silt fractions, the amount of smectite minerals, as indicated by the intensity of the 1.69 nm peak, decreased from the Ck to the Ap horizon, where they were virtualy absent. All the <0.1 μm fine clay subfractions were dioctahedral minerals, as indicated by a 060 band at 0.150 nm (not shown).

Following the Greene-Kelly test a re-expansion was observed for all the samples, except that from the parent-material (Ck horizon) (Figure 3). Thus, in the soil horizon samples (Ap, Bwss1, Bwss2 and Bwss/Ck) the smectite was beidellite. The parent material sample exhibited only a partial re-expansion, indicating that a part of the smectite was montmorillonite. Moreover, a diffraction band (2nd order) at 0.932 nm revealed interstratification of collapsed (montmorillonite) and expanded (beidellite) layers in this sample.

A precise characterization of the smectitic phase was attempted on the <0.1 μm subfractions, using decomposition of the XRD patterns.

For all the sample, the decomposition of the 1st order diffraction band has given one elementary curve only, at d-spacings between 1.701 and 1.658 nm (not shown). The prominent feature in this °2Θ region was the increase of the peak width from 1.3 °2Θ at half intensity (Ck horizon) to 2.0 °2Θ for the Ap horizon sample.

More striking differences were observed between the samples in the 16–23 °2Θ region (Figure 4). In this region the XRD diagram from the parent material sample was decomposed with three elementary curves: a broad one at 0.512 nm, attributed to I/S mixed layers with about 15% smectite layers, and two others, at 0.554 and 0.556 nm, attributed to I/S mixed layers with about 75% smectite layers (Reynolds 1980). For all the other samples, only two elementary curves were obtained by the decomposition procedure, one near 0.545 nm (0.547 nm, Bwss/Ck, 0.542 nm, Ap) that could be attributed to I/S mixed layers with about 50%

smectite layers and, one near 0.500 nm, characteristic of illitic minerals. Thus, less expandable minerals were found in the upper soil horizons than in the parent-material (Ck horizon).

XRD patterns from the K-saturated, heated to 200°C and ethylene glycol solvated samples also revealed differences between samples. The decomposition of the XRD pattern from the parent material, in the 3–13 ◇2Θ region, was achieved with four elementary curves (Figure 5). The most intense curve was at 1.617 nm, indicating fully expandable smectite with two glycol
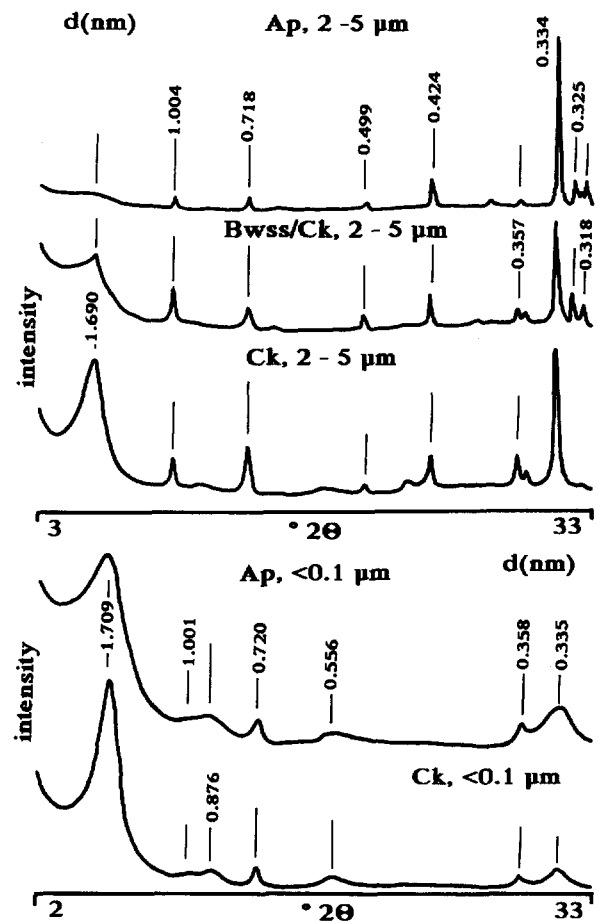

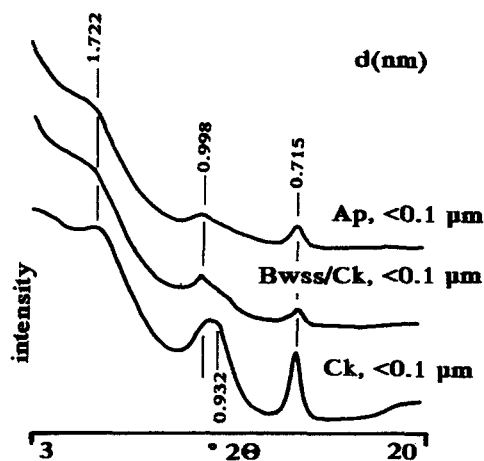Figure 2.   XRD patterns for fine silt (2–5 μm) and fine clay (<0.1 μm) subfractions. Ca-saturated, ethylene glycol solvated. CoKα radiation.

Figure 3. XRD patterns for fine clay subfractions. Li-saturated, heated to 300°C, ethylene glycol solvated. CoKα radiation.

Figure 4. Decomposed XRD patterns in the 16–23 °2θ region. ——: experimental curve, – – –: elementary computed curve, ——: best fit computed curve. Ca-saturated, ethylene glycol solvated. CoKα radiation.

layers. Thus, most of the smectite in this sample was of a low-charge type. Additional elementary curves were found at 1.323 nm, attributed to smectite with one glycol layer, 1.037 and 1.003 nm, attributed to illite and/or collapsed minerals. The XRD pattern from the Bwss/Ck sample was decomposed with three elementary curves, the most intense being at 1.460 nm. This curve was attributed to interstratified smectite layers with either one or two glycol layers. Compared to those of the parent-material sample, the intensities of the curves near 1.0 nm were strongly increased, indicating higher proportion of collapsed high-charge layers. Especially, a sharp band at 0.999 nm, not present in the parent-material sample was obtained from the Bwss/Ck sample. The three other samples (Ap, Bwss1 and Bwss2) have given quite similar decomposed XRD patterns. The most intense elementary curve was at about 1.300 nm, attributed to smectite with one glycol layer. A far less intense curve at 1.714 nm (smectite with two glycol layers) was also obtained, as well as two curves at 0.999 and 1.047 nm, respectively. Thus, a decrease of the expandability of the smectitic minerals, attributed to an increase of the layer charge, was observed from the parent material to the Bwss/Ck and then the Bwss and Ap horizon samples.

A turbostratic index (TSI) was computed with the XRD patterns from randomly oriented powder samples (Figure 6). This index was thought to be related with the amount of turbostratic defects in the stacking sequence. Reynolds (1992) has found the TSI well correlated with the proportion of smectite layers in I/S mixed-layers. According to the correlation curve, the TSI indicated 70% expandable smectite layers in the parent material sample, in good agreement with the XRD pattern from the oriented sample. For the other samples, the TSI's were only slightly changed and, indicated 60–70% expandable layers. That was more than
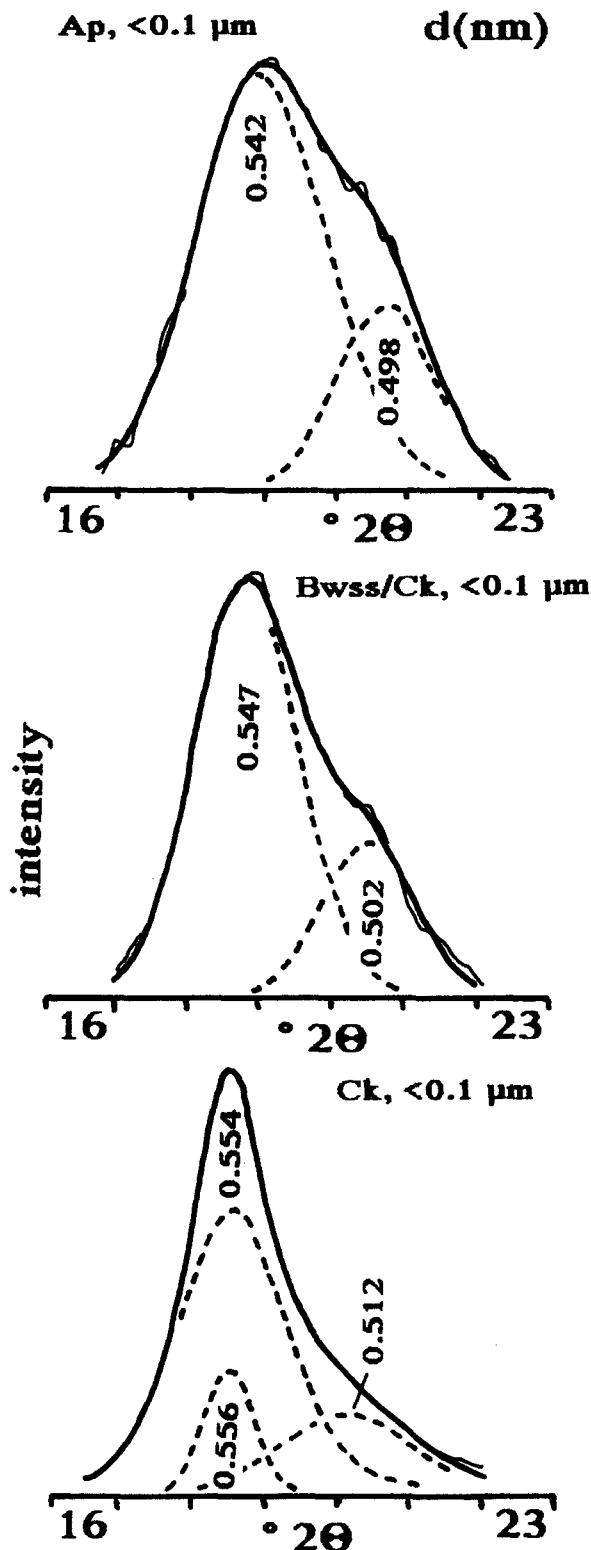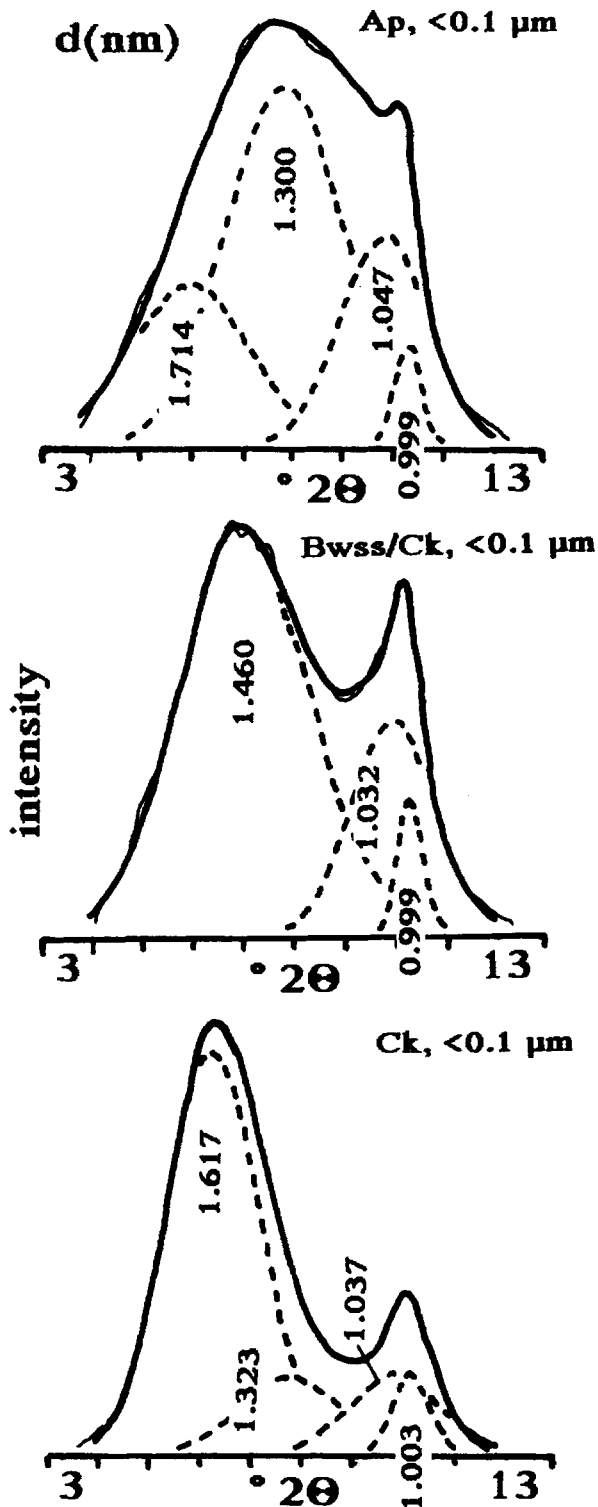
Figure 5. Decomposed XRD patterns in the 3–13 °2θ region. ——: experimental curve, – – –: elementary computed curve, ——: best fit computed curve. K-saturated, heated to 200°C, ethylene glycol solvated. CoKα radiation.
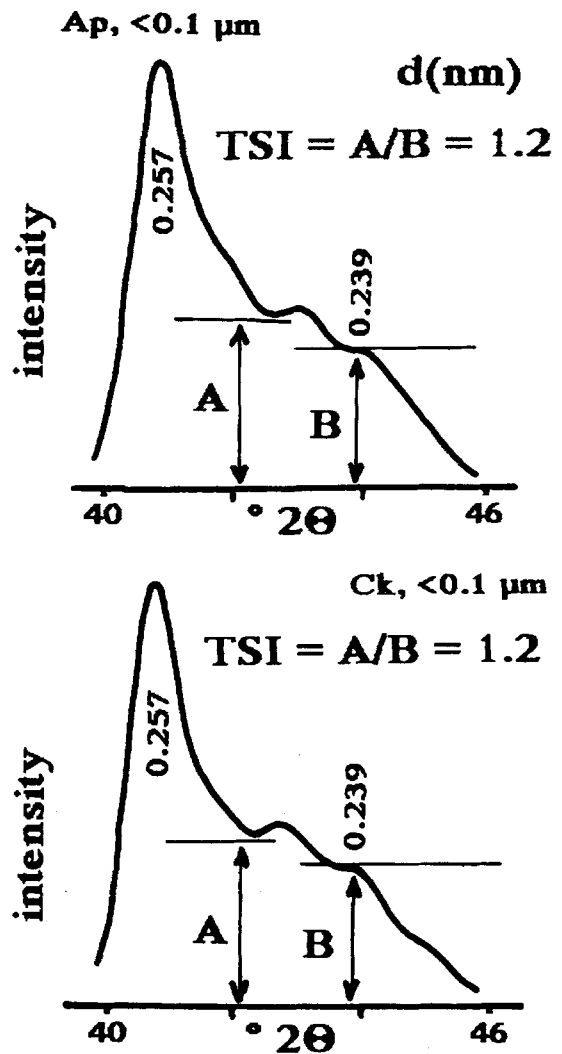

Figure 6. XRD patterns from randomly oriented powders. CoKα radiation. Definition and computation of TSI, the turbostratic index (see Reynolds 1992).

determined with the XRD patterns from oriented samples (50%) and, suggested that turbostratic defects occured not only at the expandable interfaces, but also in the stacks of collapsed layers. This also suggested that not all the layers with a 1.0 nm spacing were illitic but, in part, fully collapsed, unreexpandable smectite.

K-saturation followed by wetting and drying (WD) cycles produced various effects, according to the treated sample. After 25 WD cycles the expandability of the Bwss1, 0.1–2 μm, coarse clay sample was strongly reduced. This was indicated by the rise of the background level in the small °2θ angles region (Figure 7). As the intensities in the 16–23 °2θ region were too weak, decomposition was applied in the 9–14 °2θ region (Figure 7). The decomposition of the XRD pattern from the untreated sample has given three elementary curves,
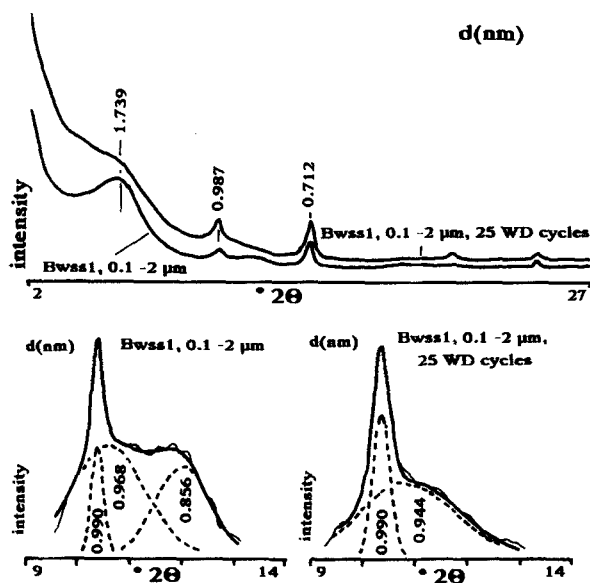
Figure 7. XRD patterns from the untreated and 25 WD cycles treated Bwss1, 0.1–2 μm samples. Ca-saturated, ethylene glycol solvated. CoKα radiation.

Figure 9. FTIR spectra for the Bwss2, <0.1 μm and Ck, <0.1 μm samples.

which were at 0.990 nm (mica), 0.968 nm (I/S mixed layers with 25% smectite) and 0.856 nm (I/S mixed layers with 90% smectite). After the WD treatment, only two elementary curves were obtained, one at 0.990 nm (mica) and the other at 0.944 nm (I/S mixed layers with 35% smectite). Thus, in the Bwss1 sample, the proportion of expandable smectite layers in the I/S
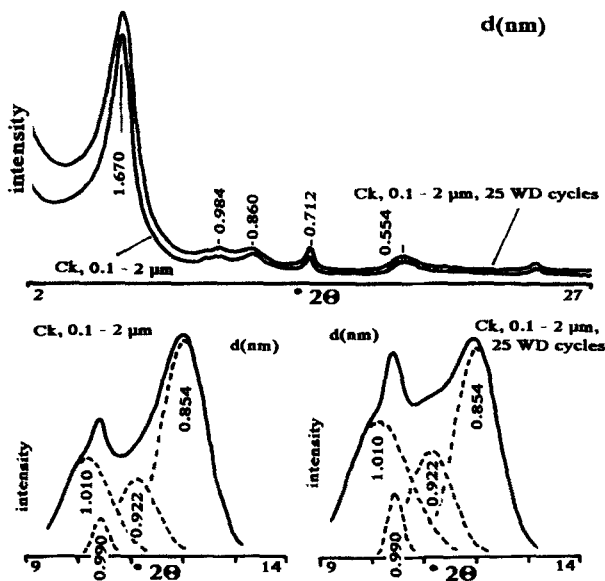

Figure 8. XRD patterns from the untreated and 25 WD cycles treated Ck, 0.1–2 μm samples. Ca-saturated, ethylene glycol solvated. CoKα radiation.
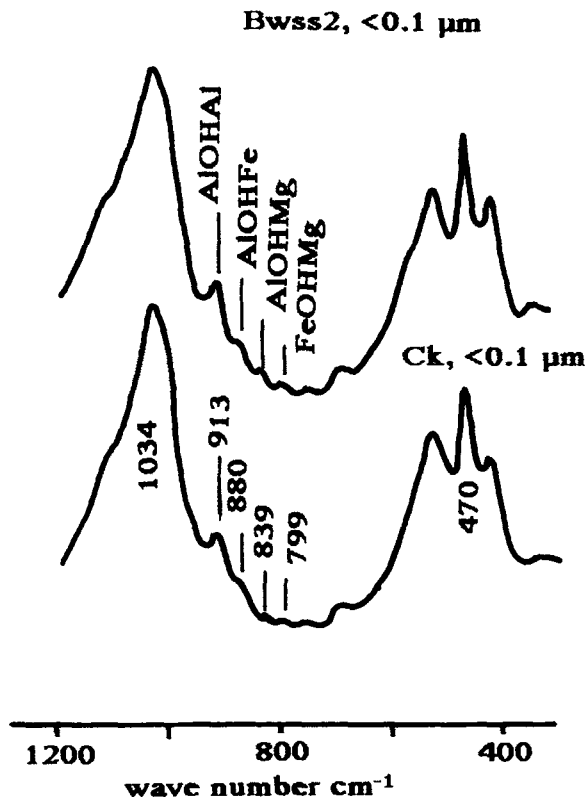
phase was reduced from 90 to 35%. The same WD treatment applied to the parent material (0.1–2 μm) sample has given less visible changes (Figure 8). Only a small proportion of the expandable layers were affected and, expandability was not dramatically decreased.

All the <0.1 μm, fine clay subfractions gave the same FTIR spectrum. This established the aluminous character of the smectite (AlOHAl band at 913 cm^{-1}). In addition, substitutions of Mg and Fe for Al in the octahedral sheet were demonstrated by the AlOHFe, AlOHMg and FeOHMg bands at 880, 839 and 799 cm^{-1}, respectively (Figure 9).

Total chemical analysis produced homogeneous results, all the <0.1 μm fine clay samples had a rather constant chemical composition (Table 3). When plotted in a [Al/(Al + Fe)] versus [Al^{IV}/(Al^{VI}/Mg^{VI})] diagram (Wilson 1987) all the sample representative points fall in the beidellite composition field (Figure 10). The K$_2$O contents were comprised between 1.50 and 1.80% of the 105°C dried samples, indicating less than 20% illite layers. The K$_2$O content was not high enough to account for the illitic phase and the I/S mixed layers with 50% illite, identified from the XRD patterns. Therefore, it is likely that the XRD patterns were those

Table 3.   Total analyses and CEC of the fine clay ($<0.1\ \mu m$) subfractions. CEC $cmol_c\ kg^{-1}$; total analyses: percent 105°C dry sample: LOI loss on ignition.

	SiO_2	Al_2O_3	Fe_2O_3	MnO	MgO	CaO	Na_2O	K_2O	TiO_2	LOI	CEC
Ap	47.20	19.35	6.76	0.12	2.10	1.80	0.10	1.50	0.75	19.30	71.60
Bwss1	46.00	19.00	8.93	0.08	2.20	2.50	0.12	1.60	0.70	18.35	80.10
Bwss2	46.80	20.30	7.08	0.06	2.20	2.00	0.15	1.50	0.95	18.79	77.80
Bwss/Ck	46.00	19.60	6.71	0.03	2.60	1.80	0.11	1.80	0.64	19.33	72.70
Ck	51.19	20.55	6.75	0.08	2.30	2.59	0.08	1.56	0.47	14.43	74.90

of interstratified high-charge, fully collapsed smectite and low-charge, expanded smectite layers rather than those of I/S mixed-layers.

CECs varied from 71.6 to 80.1 $cmol_c\ kg^{-1}$, in good agreement with the high proportion of smectite in these samples.

DISCUSSION

Particle size distribution and total chemical analysis of the bulk soil sample gave similar results for each of the soil horizons. This strongly supports the assumption that the soil parent-material was homogeneous over the soil profile, without any lithologic discontinuity. Only calcium carbonate content changed from one horizon to another, this was attributed to pedogenetic redistribution.

This Vertisol developed from a smectite-rich clayey parent-material. Although no lithologic discontinuity was observed between the parent-material and the soil horizons, a change in the clay mineralogy was demonstrated: less expandable minerals were found in the soil horizons than in the parent material (Ck horizon). The low K_2O contents and the high TSI's suggested that the partially expandable phases in the soil horizons were high-charge smectite/low-charge smectite mixed-layers, rather than true I/S mixed-layers. This was also supported by the behavior of the K-saturated, heated to 200°C and glycol solvated samples that indicated the increase of the proportion of high-charge smectite layers in the upper soil horizons. The higher proportion of collapsed layers obtained by K-saturation and WD cycles also suggested higher layer-charge for the smectites from the soil horizon than for those from the parent material. Finally, the parent-material fine clays were predominantly low-charge beidellite (and montmorillonite) whereas, high-charge beidellite was the dominant clay phase in the soil horizons.

Beidellite in Vertisols was often described as a product of mica weathering (Kounetsron *et al* 1977, Bradaoui *et al* 1987, Borchardt 1989). In this study, the soil parent-material contained mica only as a minor phase. It is unlikely that the whole mass of high-charge beidellite found in the soil horizons has derivated from mica. Even if it was, this would not explain why low-charge smectite was not still present in the soil horizons. Therefore, since the dominant clay mineral in

the parent-material was a low-charge smectite, it is reasonable to assume that it was transformed to produce the high-charge beidellite in the soil horizons. The fact that in the parent-material the smectite was, in part, montmorillonite whereas, it was entirely beidellite in the soil horizons, suggested that the increase of the layer charge was localized mainly in the tetrahedral sheet.

The transformation depicted in this study was very similar to that obtained in the experiment performed by Eberl *et al* (1993): montmorillonite was subjected to WD cycles in $KHCO_3$ solutions (pH = 8.82) at 60°C. After six cycles, the expandability of the smectite was decreased by 50%, leading to XRD pattern like that of a randomly ordered I/S mixed-layers with 50% illite. This experiment, actually, did not create illitic layers, rather it produced sufficient layer charge, so that saturation with K led to collapse of some layers to a 1.0 nm spacing. The same transformation was observed by Singer and Stoffer (1980) for saline lake sediments. In this natural system, pore-water chemistry exerted a significant control of the smectite to illite reaction: il-
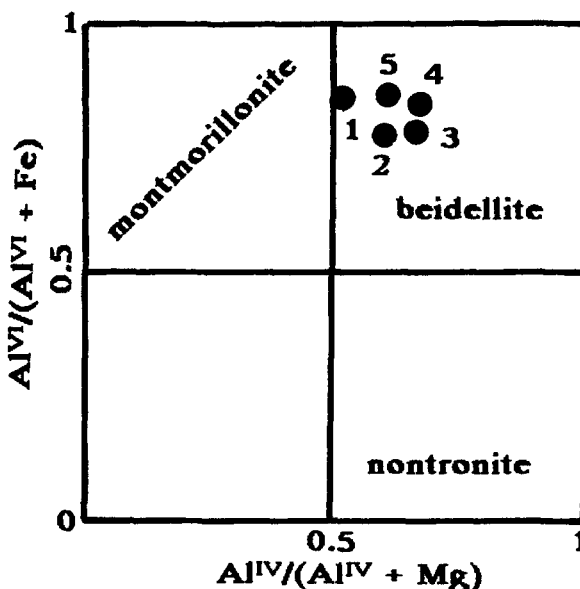

Figure 10.   Octahedral composition and relative tetrahedral charge of the fine clay ($<0.1\ \mu m$) samples. 1: Ck, 2: Bwss/Ck, 3: Bwss2, 4: Bwss1, 5: Ap.

litization (increase of layer-charge and K fixation) was favoured by increasing salinity and alkalinity. These geochemical conditions could develop in the Vertisol studied with concentration of soil solution during the drying season. The calcium carbonate associated with the clay material could also induce pHs high enough to promote desilification of montmorillonite as demonstrated by Halitim *et al* (1983).

The mechanisms that produce more Al for Si substitutions in the tetrahedral sheet (increase of the layer charge) are still unclear. Solid-state reorganization as opposed to dissolution-recrystallization process was discussed by Roberson and Lahann (1981) for hydrothermally reacted smectites. In the present study, as FTIR spectra indicated the same octahedral structure in either the low-charge or high-charge smectite clay samples, it is unlikely that complete dissolution of the low-charge layers and recrystallization of high-charge layers occurred.

CONCLUSION

The possibility of clay transformation in clay-saturated soil systems has not often been investigated. In this study, the clay minerals initially present in the parent material were dominated by smectite, a mineral formed under or near surface conditions and, expected to be stable in a Vertisol environment. In such a case the initial minerals could be expected to not transform under soil development. In the Vertisol studied, a mineralogical change was apparent, indicating the readjustment of the smectite structure to the physico-chemical conditions prevaling in the soil. Thus, high-charge bedeillite appeared to be the stable mineral phase in this environment, characterized by alkaline pH and soil solutions with high concentration of divalent cations. The high layer-charge promoted irreversible fixation of potassium from fertilizers and/or weathering of K-bearing primary minerals and, the irreversible collapse of some smectite layers.

ACKNOWLEDGMENTS

REFERENCES

Borchardt, G. 1989. Smectites. In *Minerals in Soil Environments*. 2nd ed. J. B. Dixon and S. B. Weed, eds. Madison, Wisconsin: Soil Sci. Am., 675–727.

Bradaoui, M., and P. R. Bloom. 1990. Iron-rich high-charge beidellite in Vertisols and Mollisols of the High Chaouia region of Morocco. *Soil Sci. Soc. Am. J.* **54**: 267–274.

Bradaoui, M., P. R. Blomm, and R. H. Rust. 1987. Occurrence of high-charge beidellite in a Vectic Haplaquoll of northwestern Minnesota. *Soil Sci. Soc. Am. J.* **51**: 813–818.

Eberl, D. D., B. Velde, and T. McCormick. 1993. Synthesis of illite-smectite from smectite at Earth surface temperatures and high pH. *Clay Miner,* **28**: 49–60.

Grenee-Kelly, R. 1953. The identification of montmorillonoids in clays. *J. Soil Sci.* **4**: 233–237.

Halitim, A., M. Robert, and G. Pédro. 1983. Etude expérimentale de-l'épigénie calcaire des silicates en milieu confiné. Caractérisation des conditions de son développement et des modalités de sa mise en jeu. *Sci. Géol. Mém.* **71**: 63–73.

Howard, J. J., and D. M. Roy. 1985. Development of layer charge and kinetics of experimental smectite alteration. *Clays Clay Miner.* **33**: 81–88.

Jeanroy, E. 1972. Analyse totale des silicates naturels par spectrométrie d'absorption atomique. Application au sol et à ses constituants. *Chim. Anal.* **54**: 159–166.

Kounetsron, O., M. Robert, and J. Berrier. 1977. Nouvel aspect de la formation des smectites dans les Vertisols. *C. R. Acad. Sc. Paris.* **284**: 733–736.

Lanson, B. 1993. *DECOMPXR, X-ray Decomposition Program.* Poitiers, France: ERM (Sarl).

Reynolds, R. C. 1980. Interstratified clay minerals. In *Crystal Structures of Clay Minerals and their X-ray Identification.* G. W. Brindley and G. Brown, eds. London: Miner. Soc., 249–359.

Reynolds, R. C. 1992. X-ray diffraction studies of illite/smectite from rocks, <1 μm randomly oriented powders, and <1 μm oriented power aggregates: The absence of laboratory-induced artifacts. *Clays Clay Miner.* **40**: 387–396.

Roberson, H. E., and R. W. Lahann. 1981. Smectite to illite conversion rates: Effects of solution chemistry. *Clays Clay Miner.* **29**: 129–135.

Rossignol, J.-P. 1983. Les Vertisols du nord de l'Uruguay. *Cah. ORSTOM sér. Pédol.* **20**: 271–291.

Singer, A., and P. Stoffers. 1980. Clay mineral diagenesis in two East African lake sediments. *Clay Miner.* **15**: 291–308.

SISS (Società Italiana Scienza del Suolo). 1985. *Metodi normalizzati di analisi del suolo.* Edagricole. Bologna.

Soil Survey Staff 1992. *Keys to Soil Taxonomy.* 5th Ed. 1994. Blacksburg, VA: Pochahontas Press.

Wilson, M. J. 1987. Soil smectites and related interstratified minerals: Recent developments. *Proceedings of the International clay conference, Denver.* L. G. Schultz, H. van Olphen, and F. A. Mupton, eds. The Clay Minerals Society, Bloomington, Indiana, 167–173.